



QUANTUM INTERNET ALLIANCE

D2.1 Report on high- performances ensemble- based quantum memories

Document History

Revision Nr	Description	Author	Review	Date
1	First draft	Laurat/Afzelius/de Riedmatten/ Wengerowsky/ Tittel		04.02.2022
2	Second version	Laurat/Afzelius/de Riedmatten/Tittel		14.02.2022

This project has received funding from the European Union's Horizon 2020 research and innovation programme under grant agreement No 820445.

The opinions expressed in this document reflect only the author's view and in no way reflect the European Commission's opinions. The European Commission is not responsible for any use that may be made of the information it contains.

Index

1. Abstract	5
2. Keyword list	5
3. Acronyms & Abbreviations	5
4. Introduction	6
5. Quantum memory storage-and-retrieval efficiency	7
5.1. Impedance-matched approach for solid-state memories	7
5.2. Efficiency improvement in Praseodymium doped Y_2SiO_5 (ICFO)	8
5.3. Efficiency improvement in Thulium doped $Y_3Al_5O_{12}$ (TUD)	10
5.4. High-efficiency in cold-atom based quantum memories (SU)	11
6. Long-lived solid-state quantum memories	13
6.1. Long-lived optical-coherence storage (TUD, UNIGE, ICFO)	13
6.2. Long-lived spin-wave storage (UNIGE)	15
7. Conclusion	17
8. References	18

1. Abstract

In this report we describe the progress made in QIA regarding the performances of ensemble-based quantum memories for quantum repeaters. Storage-and-retrieval efficiency and lifetime of the storage are two key parameters for quantum repeaters. We report that partners within WP2 have demonstrated close to 90% storage-and-retrieval efficiency in cold-atom-based memories, including for entanglement, and strong improvements of the state of the art for rare-earth-doped crystals via cavity enhancement, with an AFC efficiency above 60%. Maximal storage times in doped crystals have been strongly pushed, reaching values up to 100 ms for storage in spin coherence via dynamical decoupling, and up to 100 μ s for storage on optical coherence.

2. Keyword list

Ensemble-based quantum memories, storage-and-retrieval efficiency, cavity enhancement, lifetime, dynamical decoupling

3. Acronyms & Abbreviations

DoA	Description of Action
EC	European Commission
WP	Work Package
AFC	Atomic frequency comb
OD	Optical depth
DD	Dynamical decoupling

4. Introduction

WP2 develops the required technologies for quantum repeaters (QRs). A key requirement for quantum repeaters based on heralded entanglement is the need of a large storage-and-retrieval efficiency and a long storage lifetime (see Approach 1 and 2 as described in the project application). This report will describe the progress made in QIA with respect to these two figures of merit, which is the objective of Task 2.1: “Quantum node engineering” in WP2. We recall that within WP2 we investigate two physical systems for heralded entanglement QRs: rare-earth-doped crystals and laser-cooled alkali atoms.

5. Quantum memory storage-and-retrieval efficiency

This section will describe the progress made within QIA in terms of efficiency for AFC storage in rare-earth-doped crystals and in cold atomic ensembles. Common to both platforms is that quantum memories require a large optical depth (OD) – possibly after cavity-enhanced interaction with light – to work efficiently, because the incoming signal must be absorbed to be stored.

The main problem with many rare-earth ion quantum memories is that their interaction with light is weak, so it is necessary to increase the length of the crystal to reach a high OD. For a reasonable crystal length in the centimeter range, the OD is still low: for instance, in a praseodymium-doped crystal, $OD = 20 \text{ cm}^{-1}$. To target values of efficiency over 80%, we would need to resort to extremely unpractically long crystals or to multi-pass configurations. In addition, a more fundamental limitation affects the atomic frequency comb (AFC) forward retrieval efficiency. It has been shown that the maximum achievable efficiency for the retrieval of the storage pulse in the forward direction is limited to 54% by the process of re-absorption [1]. In the limit of high ODs, it can theoretically reach 100% by applying spin-wave storage and recalling the excitation backwards. A promising approach to overcome these limitations and to get high efficiencies even with low ODs, without the need to do backward retrieval, came from an article by Simon and Afzelius in 2010, where they used the concept of impedance-matched cavity [2]. This approach has been used in two platforms in QIA and it is detailed in the following subsections.

For cold-atom based ensemble, increasing the OD to large values is also a requirement to achieve large efficiency. However, a large OD can lead to loss in some circumstances. The SU group identified ways to push the OD at very large values and to reduce incoherent losses in their system. Storage of single photons in a memory and of entanglement between two quantum memories were then demonstrated with efficiency close to 90% during QIA.

5.1. Impedance-matched approach for solid-state memories

In an impedance-matched cavity, the absorption from the memory crystal inside is exactly matched to the transmission through the in-coupling mirror. If this condition is fulfilled, the efficiency can in principle reach 100% even for excited state storage. Mathematically, this condition can be expressed by stating that the reflectivity of the coupling mirror is given by reference [2]:

$$R_1 = R_2 \exp(-2\tilde{d}) = R_2 e^{-2\tilde{d}} \quad (1),$$

where R_1 is the reflectivity of the in-coupling mirror, R_2 the reflectivity of the second mirror, \tilde{d} is the optical depth of the crystal averaged over the peaks. In the case of an AFC with square teeth, this last quantity can be evaluated as $\tilde{d} = \frac{d}{F_{AFC}}$ [1], where d is the optical depth of the crystal and F_{AFC} is the finesse of the atomic frequency comb, namely the ratio between the distance among the peaks and their width. The only theoretical limitations to the efficiency with this technique are due to the finite width of the teeth of the comb, causing a dephasing, and to the intracavity losses.

A general formula to describe the efficiency of an impedance-matched cavity-assisted memory is the following [2]:

$$\eta = \left(\frac{2\tilde{d} \exp(-\tilde{d})(1-R_1)\sqrt{\eta_F}\sqrt{R_2-d_0}}{(1-\sqrt{R_1(R_2-d_0)})\exp(-\tilde{d})} \right)^2 \quad (2)$$

which, compared to Eq. (1), involves two more variables: the intra-cavity roundtrip loss in double-pass d_0 and the dephasing term η_F . This last term accounts for the finite width of the AFC peaks and, in the case of a comb with square teeth, it can be written as in reference [3]:

$$\eta_F = \text{sinc}^2\left(\frac{\pi}{F_{AFC}}\right). \quad (3)$$

It can be seen that, according to the Eq. (2), the impedance-matched efficiency η could in principle reach 100% but, in reality, we are limited by the intra-cavity losses d_0 and the finite F_{AFC} of the comb. In addition to that, once the reflectivities R_1 and R_2 of the two mirrors are fixed, this automatically sets a value of \tilde{d} . Every deviation from this value will diminish the efficiency one is able to reach.

In Fig. 1, the expected efficiency is plotted as a function of the finesse of the AFC and \tilde{d} for a given realistic double-pass loss of 8.5%. This value accounts for surface losses (from the crystal facets and the vacuum chamber windows for instance) and for the residual background absorption of the AFC.

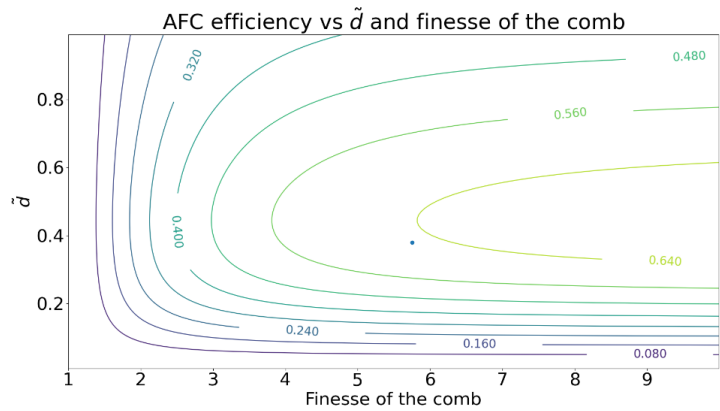


Figure 1: Expected efficiency as a function of AFC finesse and mean optical depth of the comb, for the cavity built at ICFO with $R_1 = 0.4$ and $R_2 = 0.97$, leading to an optimal value of $\tilde{d} = 0.45$.

5.2. Efficiency improvement in Praseodymium doped Y_2SiO_5 (ICFO)

ICFO developed a specific setup to implement an impedance-matched cavity quantum memory with Pr:YSO crystals. The experimental setup is shown on Fig. 2. The Pr doped crystal is placed into a cryostat and the cavity is built around it. Weak coherent pulses at the single photon level are stored in the quantum memory. The photons retrieved from the memory are emitted backward and separated from the input by a beam splitter. The mode-matching of the incoming beam to the cavity and stability of the cavity pose additional challenges. The cavity is locked using a microcontroller (Arduino Due) for 120 ms continuously during every cryostat cycle. For each cryostat cycle, 1000 laser-pulses are sent with a mean photon number of 0.2 photons per pulse during a phase of the cycle, where the mechanical vibrations are minimal.

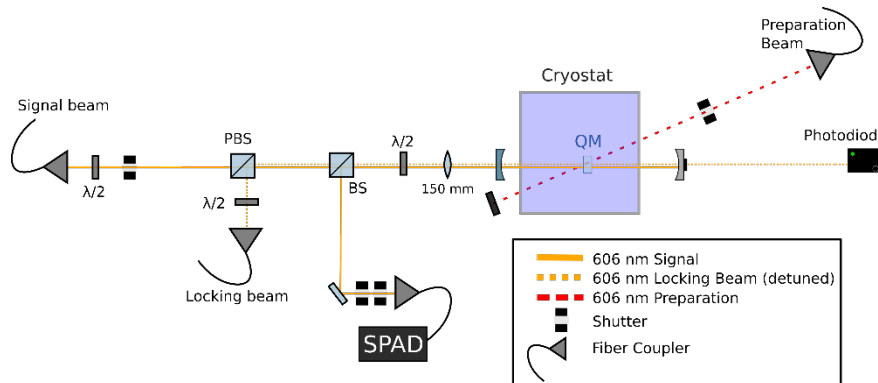


Figure 2: Simplified setup displaying the beam path and the cavity around the Pr^{3+} -doped Y_2SiO_5 crystal in the cryostat. The output of the memory is separated from the incoming light after a beam splitter and fiber-coupled to be detected by a SPAD. Locking light is inserted at the orthogonal polarization which interacts less with the Pr^{3+} -ions.

Figure 3 shows an example of atomic frequency comb. Its finesse is $F=5.8$ (3) and the effective OD is $\bar{d}=0.38$. By burning this comb inside the memory, ICFO reached 62 (2)% storage efficiency using weak coherent states with a mean photon number of 0.2 photons/pulse (Fig. 4). To the best of our knowledge, this is the highest AFC efficiency reported up-to-date.

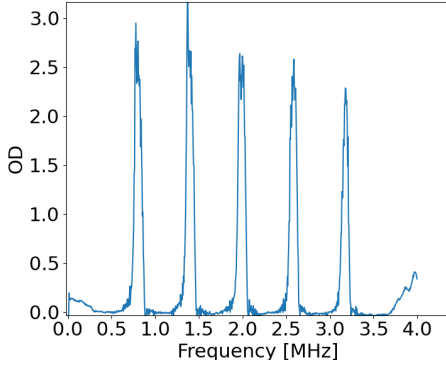


Figure 3: Atomic frequency comb with a finesse of 5.76 and an average OD of 0.38.

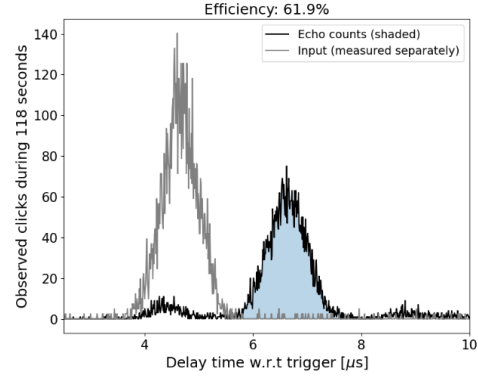


Figure 4: Efficiency measurement of storing a weak coherent state. The efficiency was $(62 \pm 2)\%$.

For this measurement, the photons' duration was about $1 \mu\text{s}$ FWHM. To store non-classical light states, it would be desirable to use shorter pulses. Figure 5 provides a measurement of the efficiency with classical pulses as a function of bandwidth. For bandwidth larger than 1 MHz, the efficiency is decreasing rapidly. The limitation in bandwidth of the memory is due to the slow-light effect that leads to a linewidth-reduction in cavity linewidth [4].

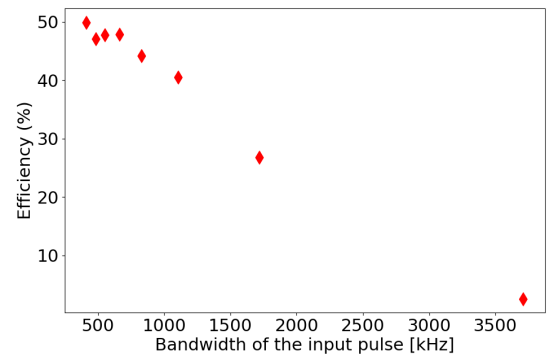


Figure 5: Memory efficiency as a function of the input pulse bandwidth, measured with classical pulses.

The blue dot in Fig. 1 represents the experimental efficiency of 61.9% for a comb finesse of 5.75. From the model, it becomes evident that a further increase in the finesse will presumably lead to an even higher efficiency.

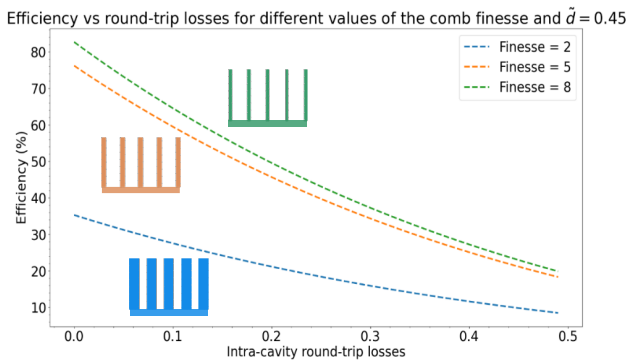


Figure 6: Expected efficiency for a fixed average OD of the comb (0.45), three different values of the AFC finesse (2, 5, 8) as a function of the intracavity round-trip losses.

Apart from that, the system is very sensitive to intra-cavity losses. If no losses were present, the model predicts an efficiency of 79%. In Fig. 6, a trend of efficiency versus intra-cavity losses is given, for three different values of the AFC finesse and a fixed value of 0.45 for the AFC average OD.

In future experiments, ICFO plans to increase these efficiencies by further optimizing the finesse and the parameter \bar{d} of the AFC and by decreasing the intra-cavity loss. ICFO also plans to store heralded single photons produced by cavity enhanced spontaneous parametric down-conversion (linewidth approximately 1 MHz) and to store time-bin qubits. Finally, it is

planned to separate the read-out of the memory from the incoming beam by a faraday rotator and a PBS or a Pockels cell in order to avoid a correction for the probabilistic splitting.

5.3. Efficiency improvement in Thulium doped $Y_3Al_5O_{12}$ (TUD)

Following the impedance-matched cavity quantum memory approach, TUD designed and implemented an AFC quantum memory for 793-nm wavelength photons using a monolithic cavity based on a Tm-doped $Y_3Al_5O_{12}$ crystal. The experimental setup is sketched in Fig. 7. This approach has been shown previously, using different rare-earth crystal hosts, to improve memory efficiency, although it has been limited to storage of classical pulses [3]. With this setup, TUD was able to improve memory efficiency and extend this method to quantum light storage.

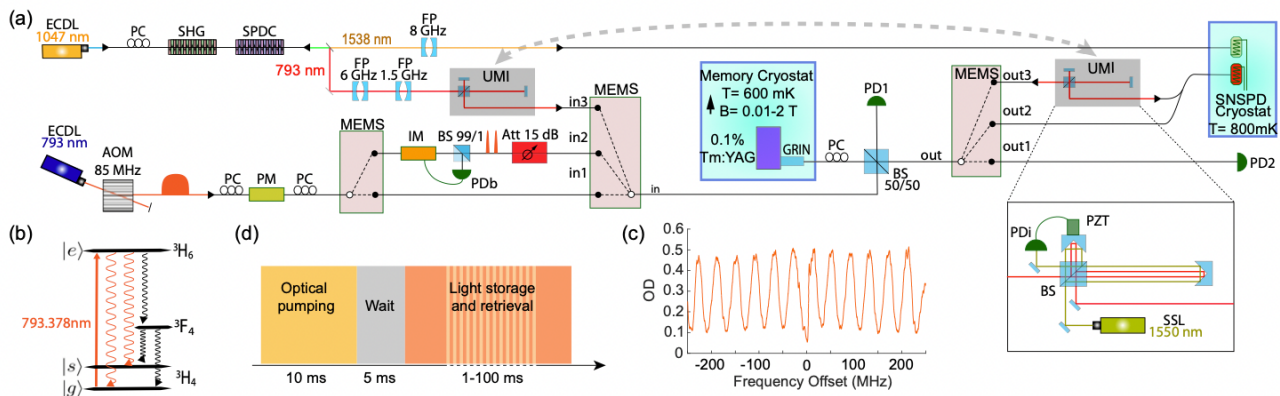


Figure 7: (a) Schematic of the experimental setup; FP: Fabry-Perot filter cavity; ECDL: external cavity diode laser; SSL: solid-state laser; SHG: second-harmonic generation; SPDC: spontaneous parametric down-conversion; FP: cavity filter; BS: beam splitter; PC: polarization controller; GRIN: gradient index lens; UMI: unbalanced Michelson interferometer; PZT: Piezoelectric actuator; Att: optical attenuator; AOM: acousto-optic modulator; PD: photodiode; MEMS; SNSPD: superconducting nanowire single-photon detectors; IM: intensity modulator; PM: phase modulator. Light from three paths was directed to an input beam splitter for AFC creation and photon storage. After reemission from the memory, the light was switched between different analyzers. (b) Level structure of Tm:YAG. (c) Example 500-MHz AFC scan of a weak read pulse across the comb. (d) Experimental duty cycle, spectral hole burning time, period of spontaneous emission, and a period for memory use.

For this sample, approximate impedance matching results in the absorption of 90% of input photons incident on the memory. With this setup a memory efficiency of $27.5 \pm 2.7\%$ over a 500-MHz bandwidth was achieved, approximately 500 times broader than previous implementations. With the increased available memory bandwidth TUD stored and recalled quantum states of light for the first time in such an impedance-matched memory. This result shows the promise of this efficiency improvement method, even for non-classical light, a necessity for quantum repeaters. The cavity enhancement results in a significant improvement over the previous efficiency in Tm-doped crystal quantum memories. The results of this single-photon storage are pictured in Fig. 8.

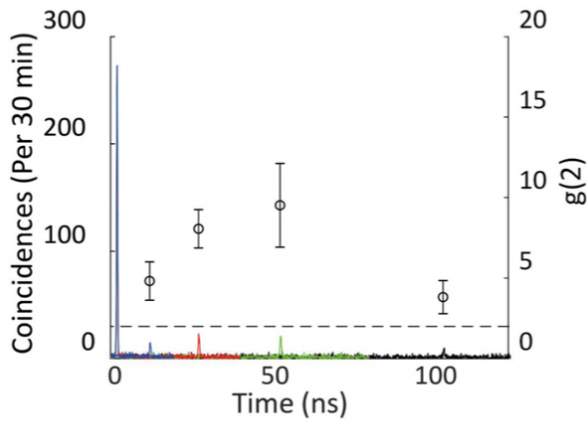


Figure 8: Time-resolved coincidence detections of a 1538-nm heralding photon and a 793-nm photon stored in the cavity memory for various different storage times. The peaks visible at each of the set storage times (10, 25, 50, and 100 ns) verify that the non-classical correlations created by SPDC persist after storage. The right-hand axis depicts the $g^{(2)}$ value for each peak with error bars multiple standard deviations above the classical limit (dashed line).

These results demonstrate progress toward efficient and faithful storage of single-photon qubits with a large time-bandwidth product for quantum networking. It was published in [5]. TUD will seek to continue this improvement in future experiments using impedance matched optical cavities by improving both cavity and memory quality factors to further raise the efficiency.

5.4. High-efficiency in cold-atom based quantum memories (SU)

For cold-atom based memory, the optical depth is also the key parameter to increase the storage-and-retrieval efficiency. However, in some circumstances, increasing the OD can lead to absorption and thereby a decrease in the achievable efficiency. To understand this scaling and OD tradeoff, the complex level structure of alkali-metal atoms has to be taken into account (Fig. 9). Hyperfine interaction in the excited state indeed introduces several levels and electromagnetically-induced transparency (EIT) features can differ from the usual, simple three level Λ -approximation. Even for cold atoms, the off-resonance excitation of multiple excited levels can have a strong effect on the medium susceptibility. These off-resonant excitations result in AC Stark shifts and effective additional ground state decoherence proportional to the control power. This decoherence rate limits the achievable transparency and therefore the storage efficiency at large OD. In Ref. [6], SU developed a full model based on the Maxwell Bloch equations and that takes into account the interaction of the signal to be stored and control field with all the excited levels (and also all the Zeeman states). Following this model, Fig. 10 provides the scaling of the memory efficiency as a function of the OD, for Cesium atoms, working either on the D2 line (as mostly done previously) and in the D1 line. In the D1 line, the excited levels are much more separated in energy and a larger efficiency can be obtained. An OD of about 500 on the D1 line can lead to a storage-and-retrieval efficiency of 90%.

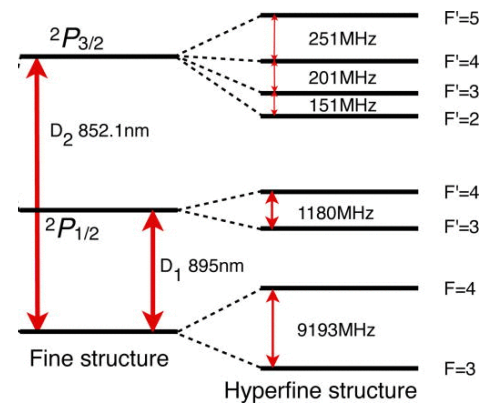


Figure 9: Fine and hyperfine structure for cesium atoms. For the D1 line, the two excited levels are separated by more than 1 GHz.

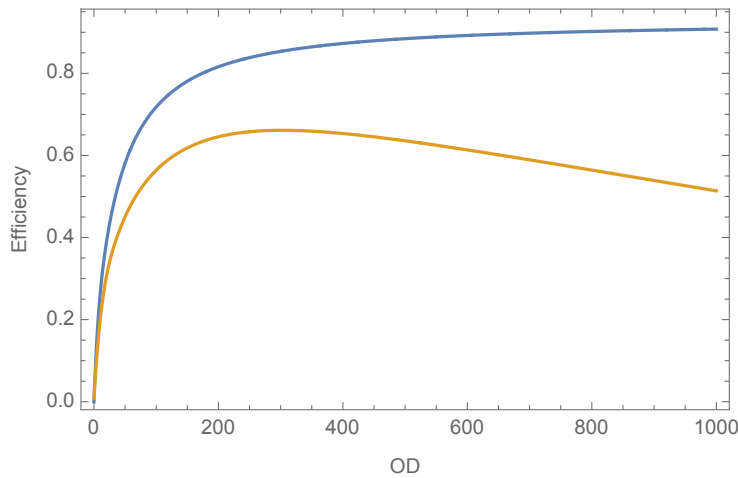


Figure 10: Storage-and-retrieval memory efficiency as a function of the OD, for cesium atoms operated on the D2 line (orange) and on the D1 line (blue). For the D2 line, the excited levels are close in energy and the off-resonant excitations lead to a trade-off. Working on the D1 line, for which the excited states are more separated, can lead to >90% efficiency for large optical depth.

In Ref. [6], SU demonstrated the storage-and-retrieval of polarization qubits with an average conditional fidelity above 99% and an efficiency around 68%. The experiment was performed at that time on the cesium D2 line, with an OD of about 300, and the obtained efficiency was the maximal achievable according to this model. Following this result, SU developed a new setup that aimed at pushing the OD higher and working on the cesium D1 line. The setup is detailed in Fig. 11. It relies on a 2.5-cm long atomic ensemble. To achieve a large OD, the magneto-optical trap (MOT) is based on two pairs of rectangular coils and on 2-inch-diameter trapping beams with a total power of 350 mW. An additional compression stage with ramping of the trapping coil currents is performed. After loading, the atoms are transferred in the F=3 ground state and polarization gradient cooling is performed. Overall, the OD on the signal transition reaches 500.

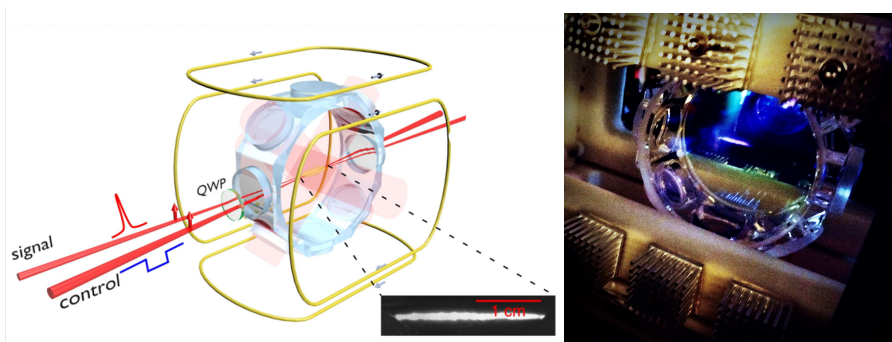


Figure 11: An elongated 2.5-cm-long magneto-optical trap of cesium atoms is obtained via two pairs of rectangular coils and large trapping beams. The right panel shows the MOT inside the vacuum chamber.

With this optimized elongated MOT, SU realized first the storage-and-retrieval of single photons and then the storage of entanglement between two quantum memories defined by two paths. This work was published in Ref. [7]. The overall experiment is shown on Fig. 12. For the storage of single photons in one memory, the maximal achieved efficiency reaches $(87 \pm 5)\%$ for an OD of about 500 (Fig. 12c). As can be seen in Fig. 12b, the single-photon character is very well preserved during the process. After demonstrating the functioning of this implementation, SU implemented the storage of single-photon entanglement between two quantum memories. A full characterization was performed and the photonic entangled state reconstructed before and after storage. The entanglement was characterized via the concurrence and the entanglement transfer, before and after storage, was measured by the ratio of the

input and output concurrences. A ratio of 88% was obtained. This number represents more than a three-fold improvement relative to previous works on entanglement storage in quantum memories.

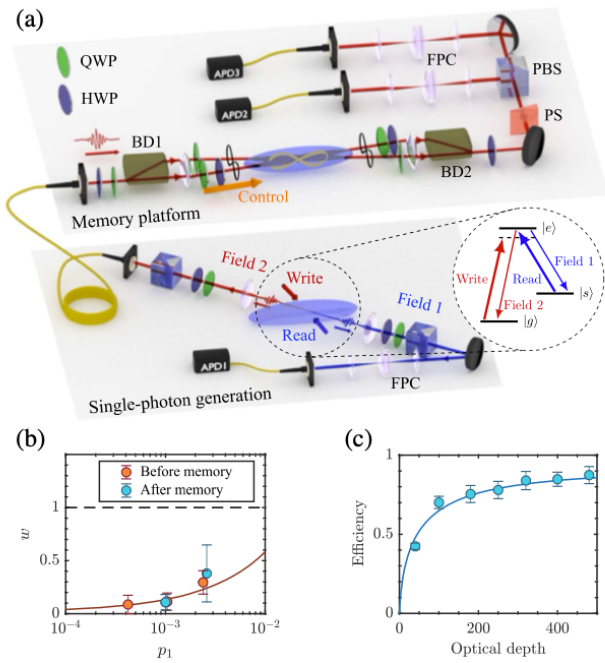


Figure 12: (a) Experimental setup. At first a single photon is generated using the DLCZ protocol in a small transverse part of the ensemble. This photon is used then for storage. (b) Suppression of the two-photon component before and after storage, for different values of excitation probability in the DLCZ generation. (c) Storage- and-retrieval efficiency for a single photon in one of the memories as a function of the OD. The efficiency reaches 87%. The line corresponds to the full model taken into account the excited levels for the cesium D1 line.

6. Long-lived solid-state quantum memories

In WP2, QIA also focuses on the extension of lifetime storage with solid-state quantum memories. Two complementary approaches have been pursued by TUD and UNIGE: extending the optical coherence time with specific crystal (TUD, UNIGE, ICFO) or implementing dynamical decoupling in spin-wave storage (UNIGE). This section will describe these two approaches and the results obtained during QIA.

6.1. Long-lived optical-coherence storage (TUD, UNIGE, ICFO)

As transferring electronic population to a ground state spin level can create significant dead time [8], leading to a reduced rate when being used as a part of a quantum repeater, TUD has followed a path aiming at using long-lived optical coherence for storage. And as this approach does not allow for read-out on demand, the targeted degree of multiplexing in their investigations is frequency, not time [9]. Then, to improve the storage times of quantum memories they employ a lesser studied crystal, Thulium-doped Yttrium Gallium Garnet (Tm:YGG), which has shown some of the longest optical coherence times among other rare-earth-ion doped crystals [10].

In this endeavor, TUD investigated the $^3H_4 \rightarrow ^3H_6$ H transition at 795.325 nm of Tm:YGG. They showed that the optical coherence time can reach 1.1 ms, and, using classical laser pulses, they demonstrated all-optical storage based on the AFC protocol up to 100 μ s with a memory decay time of 13 μ s. These results are shown in Fig. 13.

TUD also explored possibilities of how to narrow the gap between the measured value of the memory decay time and its maximum value of 275 μs . In addition, they demonstrated quantum state storage using members of non-classical photon pairs in this material. The results show the potential of Tm:YGG for creating quantum memories with long optical storage times, and open the path to building extended quantum networks [8]. For future experiments, to improve this metric, TUD will employ improved magnetic stability, a redesigned memory preparation process, and further laser stabilization to increase storage times to a length that will allow transmission of quantum information over more than 50 kilometers.

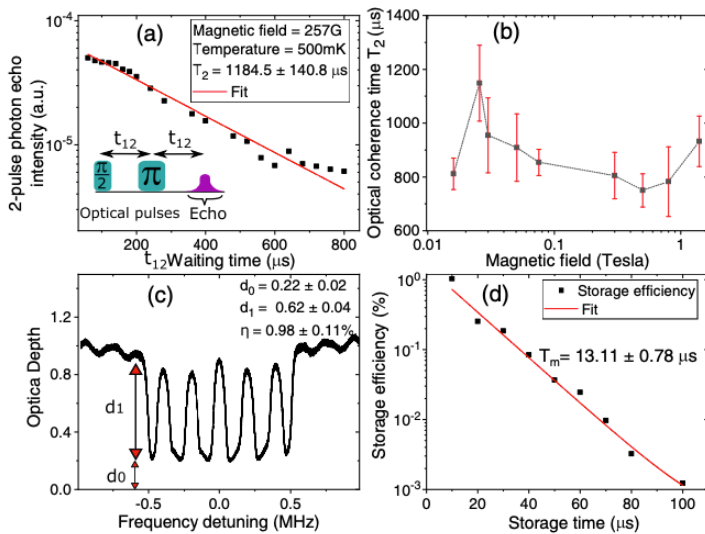


Figure 13: Storage of data in a single spectral mode. a) Exponential decay of the two-pulse photon echo signal at 257 G b) Optical coherence time T_2 as a function of magnetic field. The dashed line is a guide for the eye. c) AFC of 1 MHz bandwidth tailored for 5 μs storage time. d) Memory efficiency as a function of storage time using AFCs with finesse 2. The error bars in panels a and d are smaller than the data points.

UNIGE has also demonstrated optical storage times for up to 100 μs , with an efficiency of slightly above 5% at 100 μs in a Eu doped crystal, as shown in Fig. 14. The characteristic memory decay time T_m , defined by $\eta = \eta_0 \exp\left(-\frac{1}{\Delta T_m}\right)$, reached $T_m = 58 \mu\text{s}$ which is the longest optical AFC T_m achieved in any rare-earth crystal. The zero-delay efficiency reached $\eta_0 = 41\%$, which is only limited by the OD of the ensemble $d = 6$. Cavity enhancement should improve the efficiency further, as demonstrated by ICFO and TUD. It should also be noted that the long optical coherence in this materials should in principle allow a memory decay time T_m four times longer, showing that the current experiments have not yet reached their full potential. Using this memory UNIGE also demonstrated storage of 100 temporal modes, as explained in the D2.2 report.

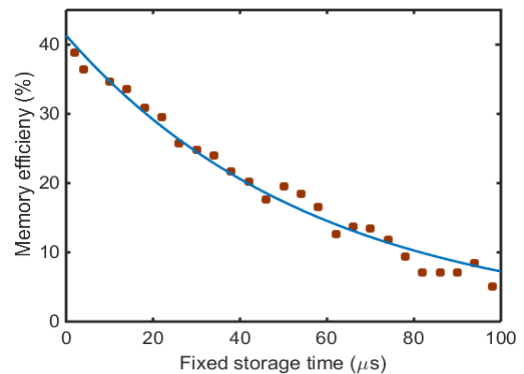


Figure 14: AFC storage efficiency as a function of the fixed-delay storage time in a Eu doped crystal. The decay constant is $T_m = 58 \mu\text{s}$ (at the $\exp(-1)$ level). The short-delay efficiency of 41% is the highest reported for a AFC memory not based on cavity enhancement.

Finally, ICFO demonstrated AFC optical storage of single photons for durations up to 25 μs in their Pr doped quantum memory. Figure 15 shows the decay of efficiency as a function of the storage time in the AFC, measured with single photons. The measured decay time are is $T_m = 23 \mu\text{s}$ (at the $\exp(-1)$ level). The efficiency measured at 25 μs is around 10 %. The single photons are heralded by the detection of a photon at telecommunication wavelengths. Following this experiment, ICFO also demonstrated the generation of entanglement between two Pr quantum memories using telecom heralding. The entanglement was stored for up to 25 μs , allowing in principle a separation of 5 km between the quantum memories [11].

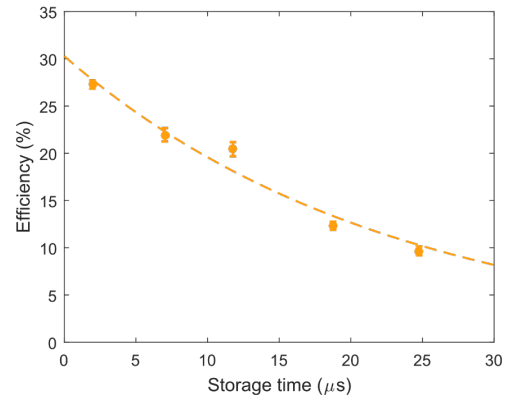


Figure 15: AFC storage efficiency of heralded single photons as a function of the fixed-delay storage time in a Pr doped crystal. The decay constant is $T_m = 23 \mu\text{s}$ (at the $\exp(-1)$ level).

6.2. Long-lived spin-wave storage (UNIGE)

UNIGE have worked on developing long-lived AFC quantum memories based on spin-wave storage. The memory device is based on $^{151}\text{Eu}^{3+}$ doped Y_2SiO_5 , as $^{151}\text{Eu}^{3+}$ is the rare-earth ion with the longest recorded spin coherence time.

To achieve AFC spin-wave storage, UNIGE currently use the Λ -system shown in Fig. 16a, where the optical states are stored on a nuclear spin transition at 46 MHz. The optical storage sequence is shown in Fig. 16b, where a train of optical input pulses are first absorbed by the AFC and then transferred into a spin-wave excitation by a strong transfer pulse. To achieve long-duration storage one must overcome both the inhomogeneous spin broadening (about 60 kHz) and the spin dephasing due to fluctuating nuclear spins in the Y_2SiO_5 crystal. To this end UNIGE uses dynamical decoupling (DD) sequences on the spin transition, as shown in Fig. 16 b-c.

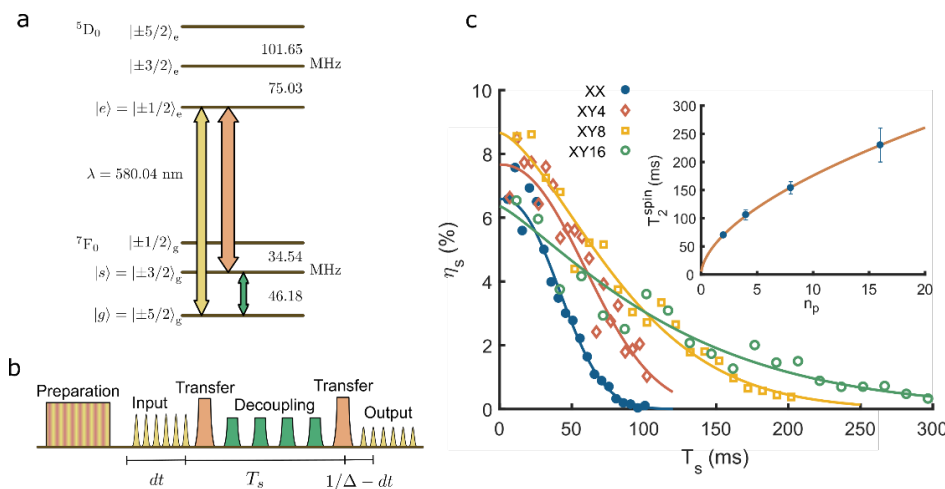


Figure 16: a) Energy level diagram of $^{151}\text{Eu}^{3+}:\text{Y}_2\text{SiO}_5$. The AFC spin-wave storage use the yellow transition for the input/output modes, the control (transfer) fields are applied on the red transition, and the spin transition used for long-duration storage is the green 46 MHz transition. b) Storage sequence showing input/output modes (yellow), optical transfer fields (red) and the RF spin decoupling sequence (green). c) Experimental result of storage efficiency as a function of storage time using different spin decoupling sequences with increasing number of pulses. Inset: spin T_2 as a function of the number of decoupling pulses.

The results show that DD sequences can significantly increase the storage time on the 46 MHz Λ -system, reaching an effective spin coherence time of $T_2^{spin} = 230 \pm 30$ ms with 16 DD pulses. The corresponding quantum node lifetime would be $230\text{ms}/2 = 115$ ms, the characteristic time when the efficiency reaches the $\exp(-1)$ level of the initial efficiency at very short storage times. Note that the T_2^{spin} closely follows the expected power law dependence $n^{2/3}$ as a function of decoupling pulses n . Similar results were achieved on the 35 MHz Λ -system, where UNIGE showed up to $T_2^{spin} = 530$ ms, but for a larger number of pulses [12]. The current 46 MHz Λ -system has about twice as long coherence time at $n = 1$, hence one can reach longer storage times with less decoupling pulses. This is one of the reasons UNIGE currently concentrates efforts on this Λ -system, as noise at the single photon level is mainly caused by the decoupling pulses.

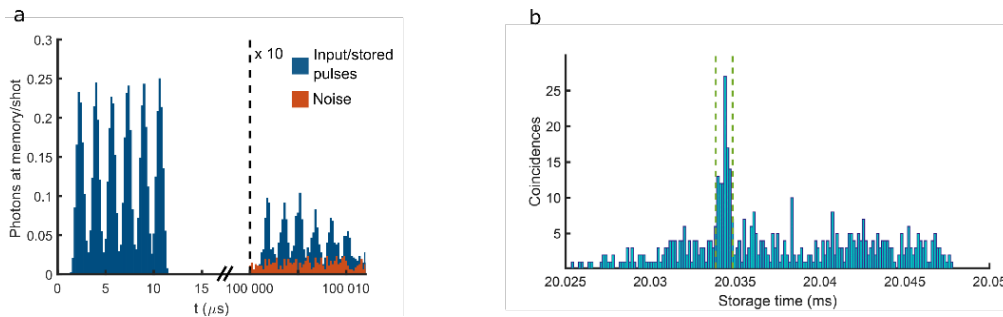


Figure 17: a) Photon counting histogram when storing weak coherent states during 100 ms with about 1.1 photon per temporal input mode. The red histogram shows the noise when applying the complete memory sequence, but with vacuum states as input modes. b) Example of two-photon coincidence detection histogram in a AFC-DLCZ experiment, where one of the photons has been stored for a duration of 20 ms in the spin state. Counts within the temporal gate shown by the dashed green lines was used to calculate the second-order quantum correlation function.

Storage at the single photon level is challenging due to noise created during the spin-wave storage and the read-out with the strong optical transfer pulse. UNIGE is currently the only group in the world that applies spin DD sequences to single-photon-level storage due to this challenge, although it is generally admitted that long-duration storage requires such techniques. State-of-the-art results of single-photon-level storage with DD sequences in AFC spin-wave memories are shown in Fig. 17. In Figure 17a we show weak coherent state storage of six temporal modes [13], with each input modes containing 1.1 photon in average, for a total duration of 100 ms using $n = 16$ pulses (XY-16). The signal-to-noise ratio (SNR) is 2.5 ± 0.2 at 100 ms, while it is 7.4 ± 0.5 for a shorter storage time of 20 ms ($n = 4$). The noise is caused by imperfections in the DD sequence, which populates the storage state with population that is causing spontaneous emission at the read-out of the memory. The noise per mode is of the order of 5 to 10×10^{-3} , which the probability to detect a noise photon at the output. The storage efficiency is currently limited to 2.6% at 100 ms, and 7.4% at 20 ms. Clearly, significantly larger SNR could be achieved with the same noise numbers for a higher memory efficiency.

UNIGE is also working towards exploiting the long storage times to demonstrate long-duration storage of quantum correlations, based on the AFC-DLCZ scheme, which so far has been demonstrated with a storage time of about 1 ms at UNIGE in 2017 [14]. In Figure 17b, we show an example of a coincidence measurement between two photons, of which one was stored during 20 ms in the $^{151}\text{Eu}^{3+}$ doped Y_2SiO_5 crystal. The second-order cross-correlation function $g_{si}(0)$ calculated using the indicated temporal gate gives $g_{si}(0) = 5.2 \pm 0.7$, showing quantum correlations after 20 ms storage. The AFC-DLCZ measurements had to be interrupted end of August 2021 due to relocation of the UNIGE labs to a new building. It is expected that experiments can be resumed in January 2022 after moving and rebuilding the labs in the new building.

7. Conclusion

In this report we have presented storage-and-retrieval efficiency improvements in solid-state memories via cavity enhancement, with values up to 62% in fixed-delay AFC with weak coherent states, and efficiency close to 90% in cold atom-based quantum memories via on-demand EIT both for single-photon storage and entanglement storage between two quantum memories. This last result was obtained via a very large optical thickness and the use of adequate optical transitions on the cesium D1 line. The result with cold-atom ensembles obtained at SU fulfills M2.7, and constitutes the state-of-the-art efficiency for a quantum memory. The limitation of the current AFC efficiency was carefully analysed, showing that there exist a strategy that should allow an increase in efficiency given a realistic reduction on the intra-cavity losses in the implementation.

The second figure of merit that was studied is the storage time of solid-state quantum memories. Two different strategies were explored, corresponding to different potential implementations of quantum repeaters. We have presented improvements for both strategies. For fixed storage times, we achieved a storage time up to 100 μs , with a 13 μs memory decay time, in long-lived optical coherence by using specific Tm doped crystal featuring an optical T_2 time in excess of 1 ms and a wide inhomogeneous broadening of 56 GHz allowing large frequency multiplexing. We also achieved a record memory decay time of 58 μs in a Eu doped crystal. Finally, single photons and entanglement were stored for to 25 μs in a Pr doped crystal. For on-demand storage time, we achieved a spin T_2 time up to 230 ms by using dynamical decoupling. Due to the relocation of UNIGE labs, it has not yet been possible to demonstrate non-classical correlations for this large storage time (M2.8).

8. References

- [1] M. Afzelius, C. Simon, H. de Riedmatten and N. Gisin, *Phys. Rev. A* 79, 052329 (2009).
- [2] M. Afzelius and C. Simon, *Phys. Rev. A* 82, 022310 (2010).
- [3] P. Jobez, I. Usmani, N. Timoney, C. Laplane, N. Gisin and M. Afzelius, *New J. Phys.* 16, 083005 (2014).
- [4] M. Sabooni, Q. Li, S. Kröll and L. Rippe, *Phys. Rev. Lett.* 110, 133604 (2013).
- [5] J.H. Davidson, P. Lefebvre, J. Zhang, D. Oblak, and W. Tittel, *Phys. Rev. A* 101, 042333 (2020).
- [6] P. Vernaz-Gris, K. Huang, M. Cao, A.S. Sheremt, and J. Laurat, *Nature Commun.* 9, 363 (2018).
- [7] M. Cao, F. Hoffet, S. Qiu, A. S. Sheremet, J. Laurat, *Optica* 7, 1440 (2020).
- [8] M. F. Askarani, A. Das, J.H. Davidson, G.C. Amaral, N. Sinclair, J.A. Slater, S. Marzban, C.W. Thiel, R.L. Cone, D. Oblak, and W. Tittel, *Phys. Rev. Lett.* 127, 220502 (2021).
- [9] N. Sinclair, E. Saglamyurek, H. Mallahzadeh, J.A. Slater, M. George, R. Ricken, M.P. Hedges, D. Oblak, C. Simon, W. Sohler, and W. Tittel, *Phys. Rev. Lett.* 113, 053603 (2014).
- [10] M. Businger, A. Tiranov, K.T. Kaczmarek, S. Welinski, Z. Zhang, A. Ferrier, P. Goldner, and M. Afzelius, *Phys. Rev. Lett.* 124, 053606 (2020).
- [11] D. Lago-Rivera, S. Grandi, J. V. Rakonjac, A. Seri, and H. de Riedmatten, *Nature* 594, 37 (2021).
- [12] A. Holzäpfel, J. Etesse, K. T. Kaczmarek, A. Tiranov, N. Gisin, and M. Afzelius, *New J. Phys.* 22, 063009 (2020).
- [13] A. Ortu, A. Holzäpfel, J. Etesse, and M. Afzelius, [arXiv:2109.06669](https://arxiv.org/abs/2109.06669)
- [14] C. Laplane, P. Jobez, J. Etesse, N. Gisin, and M. Afzelius, *Phys. Rev. Lett.* 118, 210501 (2017)